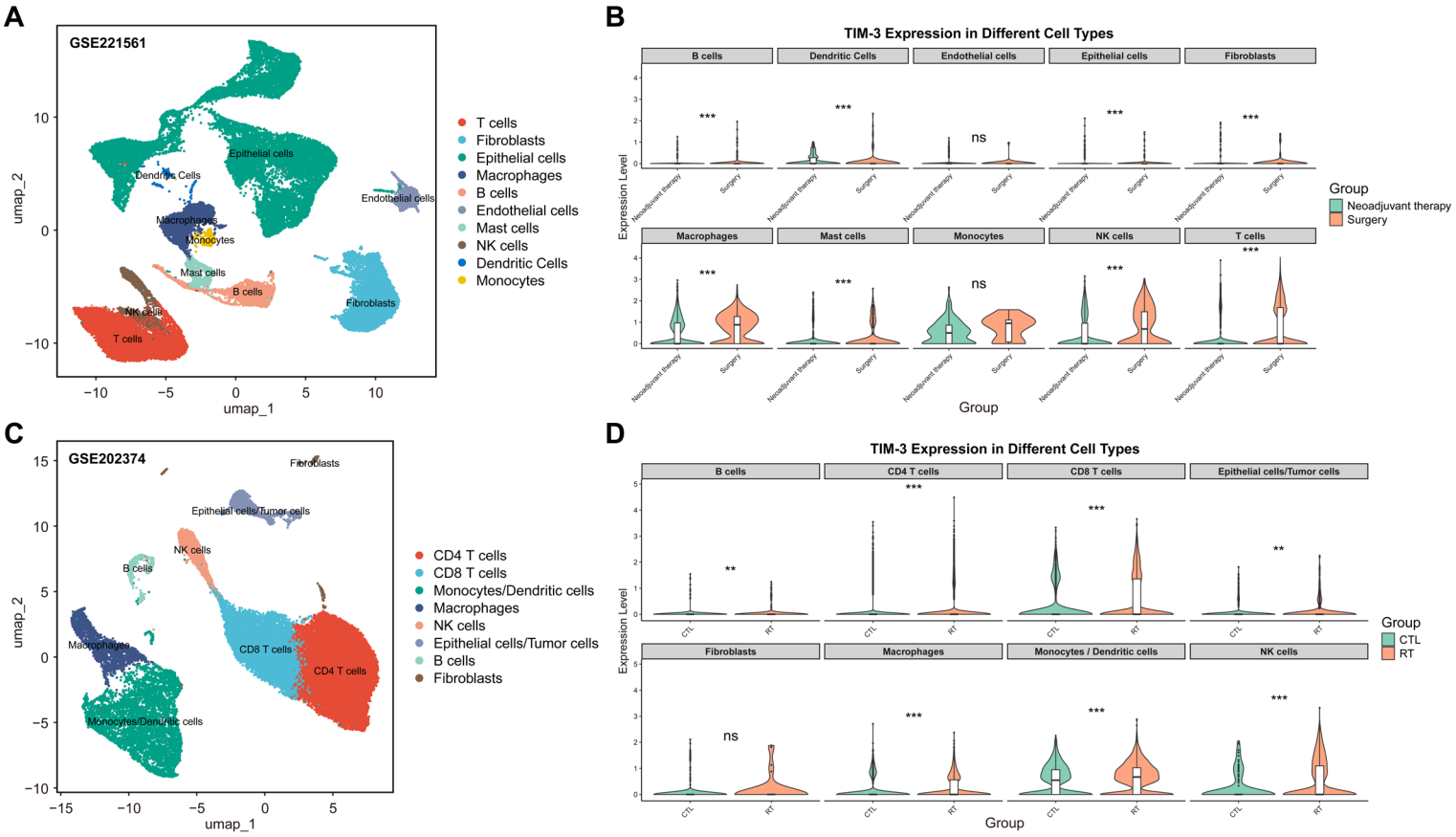

Figure S1. (A) UMAP visualization of single cells from esophageal squamous cell carcinoma before and after radiotherapy (GSE221561), with colors representing different cell types as indicated. (B) Expression levels of TIM-3 across different cell types in the GSE221561 dataset before and after radiotherapy. (C) UMAP visualization of single cells from renal cell carcinoma before and after radiotherapy (GSE202374), with colors representing different cell types as indicated. (D) Expression levels of TIM-3 across different cell types in the GSE202374 dataset before and after radiotherapy. * $p < 0.05$; ** $p < 0.01$; *** $p < 0.001$

Supplementary materials and methods

Single-cell RNA-seq data analysis: Public single-cell RNA-seq datasets for esophageal squamous cell carcinoma (GSE221561, including 7 patients receiving neoadjuvant therapy and 2 undergoing surgery alone) and renal cell carcinoma (GSE202374, comparing radiotherapy-treated resected tumors with nephrectomy-only controls) were downloaded from the Gene Expression Omnibus (GEO) database. Raw data were processed and analyzed using the Seurat package in R (Version 4.4.1). Cells with < 200 or > 5,000 detected genes and mitochondrial gene percentage > 10% were excluded as low-quality

cells. Gene expression matrices were normalized using the LogNormalize method and scaled to regress out confounding sources of variation. Principal component analysis (PCA) was performed on highly variable genes, and the first [e.g., 15] principal components were used for t-distributed stochastic neighbor embedding (t-SNE) or uniform manifold approximation and projection (UMAP) dimensionality reduction. Cell clusters were identified using a shared nearest neighbor (SNN) modularity optimization-based clustering algorithm with a resolution parameter of [e.g., 0.5]. Cell types were annotated based on canonical marker genes or according to the original study's annotations. Differential expression analysis of TIM-3 between pre- and post-radiotherapy samples across different cell types was performed using the Wilcoxon rank-sum test. Statistical significance was defined as *$p < 0.05$, **$p < 0.01$, and ***$p < 0.001$. Visualization of UMAP plots and feature plots was generated using Seurat's visualization functions.

Table S1. Sequence of primers.

Gene	Forward	Reverse
β-actin	CATGTACGTTGCTATCCAGGC	CTCCTTAATGTCACGCACGAT
TIM-3	TTGGACATCCAGATACTGGCT	CACTGTCTGCTAGAGTCACATTC
MYB	CGCAGCCATTCAGAGACACT	GCTGCATGTGTGGTTCTGTG
GZMB	CCCTGGGAAAACACTCACACA	GCACAACTCAATGGTACTGTCG
TNFa	CCTCTCTCTAATCAGCCCTCTG	GAGGACCTGGGAGTAGATGAG
IFNG	TCGGTAACTGACTTGAATGTCCA	TCGCTTCCCTGTTTTAGCTGC
PRF	GTGGGACAATAACAACCCCAT	TGGCATGATAGCGGAATTTTAGG

Table S2. Sequence of siRNAs.

siRNA	Sense	Antisense
siTIM-3 (NC)	UUCUCCGAACGUGUCACGUTT	ACGUGACACGUUCGGAGAATT
siTIM-3 (1)	GCUUAAAUUCUGUAUCUUCUCTT	GAGAAGAUACAGAAUUUAAGCTT
siTIM-3 (2)	UGUAUUCCACUUCUGAGGACCTT	GGUCCUCAGAAGUGGAAUACATT
siTIM-3 (3)	GCUAGAGUCACAUUCUCUAUGTT	CAUAGAGAAUGUGACUCUAGCTT

Table S3. The antibodies information used in this study.

Antibody	Source	Cat No.	Reactivity	Application in this study
TIM-3 pAb	Abmart, China	PQA1998S	Human, Mouse	WB, IHC, mIF
NKp46 pAb	Abmart, China	TD7599S	Mouse	IHC, mIF
MYB pAb	Proteintech, China	7800-1-AP	Human, Mouse	WB, IHC, mIF
β-actin mAb	Proteintech, China	66009-1-Ig	Human	WB
CD56 pAb	servicebio, China	GB112671-100	Human	IHC, mIF
CD8 mAb	Proteintech, China	66868-1-Ig	Mouse	IHC
KI67 pAb	Proteintech, China	28074-1-AP	Mouse	IHC
Anti-mouse Tim-3	BioXCell, America	BE0115	Mouse	In vivo experiments
Anti-mouse NK1.1	BioXCell, America	BE0036	Mouse	In vivo experiments
Anti-mouse IgG2a	BioXCell, America	BE0085	Mouse	In vivo experiments